

Delivery of siRNA and other macromolecules into skin and cells using a peptide enhancer

Tracy Hsu and Samir Mitragotri¹

Department of Chemical Engineering, University of California, Santa Barbara, CA 93106

Edited by Robert Langer, Massachusetts Institute of Technology, Cambridge, MA, and approved July 25, 2011 (received for review October 27, 2010)

Delivery of macromolecules into cells and tissues such as skin is a major challenge. This obstacle poses a particular challenge for the delivery of siRNA where cellular and tissue level transport barriers need to be overcome. siRNAs are potential therapeutics for various dermatological diseases including psoriasis, atopic dermatitis, and cancer; however, their utility is limited by their low absorption across the stratum corneum (SC) and into viable cells of skin. Here, we address this challenge using a peptide identified by phage display termed skin penetrating and cell entering (SPACE) peptide. In vitro studies indicated that the SPACE peptide, when conjugated to cargoes such as small molecules and proteins, was able to facilitate their penetration across the SC into epidermis and dermis. The peptide also exhibited increased penetration into various cells including keratinocytes, fibroblasts, and endothelial cells, likely through a macropinocytosis pathway. The ability of SPACE peptide to deliver siRNA was tested in vivo using two targets, interleukin-10 and GAPDH. Conjugation of the peptide to siRNA led to their enhanced absorption into skin and knockdown of corresponding protein targets.

cell-penetrating peptide | dermatology | drug delivery | topical | transdermal

Skin, the largest organ of the human body, is a host to numerous dermatological diseases, which collectively represent a large category of human health conditions (1–3). Accordingly, successful delivery of therapeutics, specifically macromolecules such as siRNA, into skin has become a topic of active research and development (4–6). The goal of topical siRNA delivery, however, is extremely challenging and with some exceptions has been very difficult to accomplish (7, 8). The primary challenge is poor skin penetration of macromolecules (5). Among various physico-chemical methods proposed to enhance penetration of macromolecules (9–12), peptide carriers have emerged as a potential candidate owing to their simplicity of use, diversity, and potential ability to target cellular subtypes within the skin. Several peptides including TAT, polyarginine, megalin, and penetratin, which were initially identified for delivering drugs into the cytoplasm of cells, have been tested for penetration across the stratum corneum (SC) and a few have shown some efficacy in delivering small molecules into epidermis (13–16). In contrast, only one peptide, TD-1, has been specifically discovered to penetrate the SC and possessed the ability to enhance systemic uptake of topically applied drugs (17). Although several peptides are known to penetrate cellular membranes and a few to permeabilize the SC, peptides that simultaneously enhance the penetration of macromolecules across the SC and permeabilize the membrane of viable epidermal and dermal cells have not been reported. Here, we report on the identification and utility of one such peptide.

Results

Peptides that penetrate the SC were identified using in vitro phage display (Fig. 1A). Five rounds of selection led to narrowing down the display library (Fig. 1B). One sequence, AC-TGSTQH-QCG, appeared in high frequency in higher rounds and was labeled a skin permeating and cell entering (SPACE) peptide. A second

sequence (AC-HSALTKH-CG) also appeared in high frequency. In a separate experiment, phage screening was performed to isolate phage that localized in the dermis (*S1 Materials and Methods*). After five rounds of screening, the sequence AC-KTGSNHQ-CG was found to localize specifically in the dermis. Owing to the similarity of this sequence with the SPACE peptide sequence, the SPACE peptide was selected for further studies. Fluorescently labeled phage clones displaying SPACE peptide exhibited small but detectable penetration into skin (Fig. S1A). In contrast phage clones exhibiting a scrambled peptide sequence (AC-THGQTQSCG) exhibited only superficial penetration (Fig. S1B).

The SPACE peptide, when removed from the phage, also penetrated into the skin (Fig. 1C). Consistent with the observations made with the entire phage, SPACE peptide was found to localize strongly in the dermis. No significant penetration of the control peptide was observed (Fig. 1D). SPACE peptide was also able to carry macromolecular cargoes across porcine SC. For example, streptavidin, when conjugated to biotinylated SPACE peptide, permeated well beyond the SC and some localization of streptavidin was found in the epidermis and dermis (Fig. 1E). Streptavidin not conjugated to SPACE peptide exhibited minimal penetration into epidermis (Fig. 1F). SPACE peptide-mediated transport appears to be dependent on the cargo size. Specifically, SPACE peptide, when conjugated to streptavidin-coated quantum dots, led to detectable but much smaller transport (Fig. S1C). No significant penetration of quantum dots conjugated to the control peptide was observed (Fig. S1D).

SPACE peptide also permeated across human skin and exhibited penetration comparable to that found in porcine skin (Fig. S1E and F). When observed from the top, high localization of the SPACE peptide within the corneocytes was found whereas no significant penetration of the control peptide was observed (Fig. S1G and H). Experiments with isolated human SC revealed that the SPACE peptide binds to corneocyte proteins, most likely to keratin (Fig. S2A and B). FTIR spectroscopy studies also confirmed the effect of SPACE peptide on keratin. Specifically, SC exposed to SPACE peptide exhibited changes in the FTIR spectrum, indicative of structural changes in keratin (Fig. S2C). The control peptide had no significant effect on protein structure in FTIR compared to that seen in the absence of any peptide (Fig. S2D and Fig. S3). FTIR also showed that the SPACE peptide had no detectable effect on SC lipids (Fig. S2E and F). Neither a change in the area of the symmetric CH₂ stretching peak nor a shift in center frequency was found indicating that the SPACE peptide did not induce extraction or fluidization of SC lipids (18). Consistent with the FTIR data, exposure to SPACE peptide did not induce a significant change in skin's electrical conductivity (Fig. S4). Specifically, the electrical conductivity

Author contributions: T.H. and S.M. designed research; T.H. performed research; T.H. contributed new reagents/analytic tools; T.H. and S.M. analyzed data; and T.H. and S.M. wrote the paper.

The authors declare no conflict of interest.

This article is a PNAS Direct Submission.

¹To whom correspondence should be addressed. E-mail: samir@engineering.ucsb.edu.

This article contains supporting information online at www.pnas.org/lookup/suppl/doi:10.1073/pnas.1016152108/-DCSupplemental.

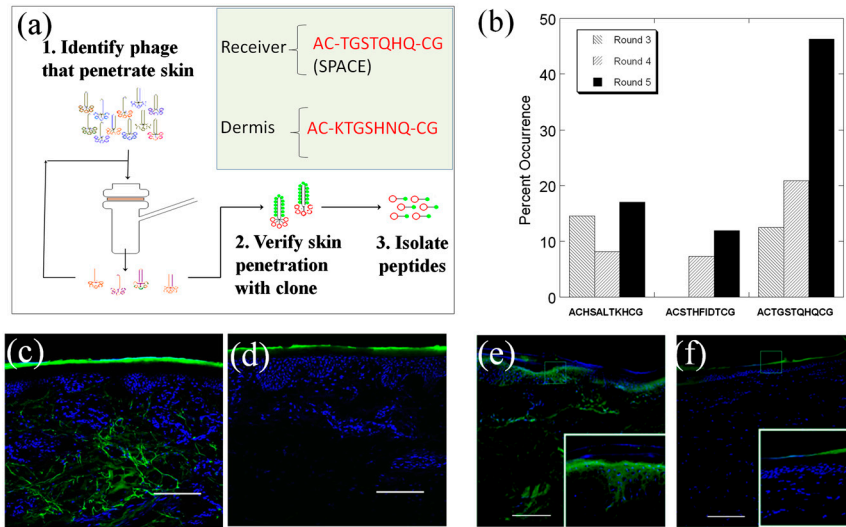


Fig. 1. The identification of skin penetrating peptides through in vitro phage display in porcine skin. (A) Phage library was applied in the donor compartment of an FDC. Phage found to penetrate through skin into the receiver compartment were collected, amplified, and used for the subsequent rounds of screening. The skin penetrating ability of individual clones was confirmed through diffusion experiments and confocal microscopy. To confirm the peptide's ability to penetrate skin, the peptide was isolated from the phage and its penetration into skin was confirmed visually through confocal microscopy. (B) Percentage of occurrence for each high frequency peptide sequence from rounds 3 through 5 of the phage display screen. (C and D) Confocal microscopy images of the skin penetration profiles of SPACE and control peptide into porcine skin, respectively. (E and F) Skin penetration profiles of Alexa Fluor 488 labeled streptavidin conjugated to biotinylated SPACE peptide and Alexa Fluor 488 streptavidin alone, respectively. *Insets* show zoomed in views of the sections highlighted in the main images. Scale bar: 200 μm .

ity of skin increased by about 1.7(+/-0.6)-fold after 24 h incubation with the SPACE peptide. This enhancement, though higher than that observed for the control peptide, was relatively modest. Similarly, coincubation of SPACE peptide with inulin, a large hydrophilic molecule led to only a modest increase in its permeability (Fig. S4), indicating that the SPACE peptide is primarily effective in enhancing permeation of conjugated but not coadministered cargoes.

Having confirmed the ability of the SPACE peptide to penetrate the SC, we next investigated its ability to penetrate into viable cells including keratinocytes, fibroblasts, and endothelial cells (HUVECs) in cell cultures and found significant penetration into all cell lines (Fig. 2 A–F and G shows a magnified view of SPACE peptide internalization in keratinocytes). In all cases, the extent of internalization of SPACE peptide was higher than that of control peptide indicating that cellular penetration occurred in a sequence-specific manner (Fig. 2H). SPACE peptide also exhibited internalization in breast cancer cells (MDA-MB-231, Fig. S5 A–C). The ability to penetrate all tested types of cells suggest that the mode of entry into cells for SPACE peptide is through a pathway that is common to all studied cell lines and not because of a particular membrane protein unique to keratinocytes.

To determine the potential mechanism of cellular penetration for SPACE peptide, the effect of several endocytosis inhibitors including incubation at 4°C on internalization was tested in human keratinocytes (Fig. 3A). Incubation at 4°C significantly reduced internalization of SPACE peptide (about 5% uptake compared to that at 37°C) as well as the control peptide indicating that both enter cells through an active mechanism. The potential mechanism for cellular penetration was further confirmed by the use of deoxy-D-glucose, which also resulted in the reduction of internalization of both peptides (~52%). To further assess the nature of the active uptake, cells were incubated with the clathrin-mediated endocytosis inhibitor chlorpromazine and the caveolae-mediated endocytosis inhibitor nystatin. Neither of them reduced the cellular internalization of SPACE peptide or the control peptide. Finally, we tested the effect of a macropinocytosis inhibitor 5-(N-ethyl-N-isopropyl) amiloride (EIPA). Exposure of cells to EIPA resulted in approximately 50% reduction

in SPACE internalization. In contrast, EIPA had no effect on control peptide internalization. Collectively, these results suggest that macropinocytosis plays a major role in the internalization of SPACE peptide, a conclusion that is shared by other cell-penetrating peptides in the literature (19, 20). Studies have reported that cargoes that are internalized by macropinocytosis are often not colocalized with endo/lysosomes implying that their entry into degrading lysosomal compartment can be potentially avoided (21, 22). MTT, 3-(4,5-dimethylthiazol-2-yl)-2,5-diphenyl tetrazolium bromide, assays on keratinocyte cultures revealed

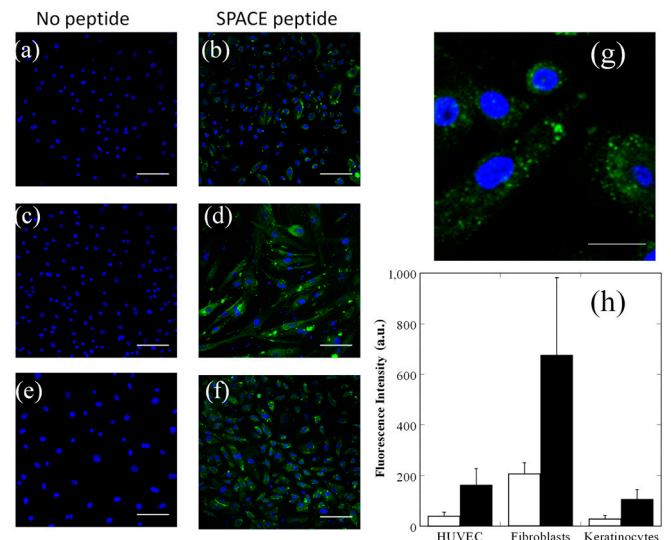


Fig. 2. Cellular penetration of SPACE peptide into various cell lines. (A, C, and E) Confocal images of cells treated with no peptide. (B, D, and F) Cells incubated with fluorescently labeled SPACE peptide for 24 h. (A and B) Human keratinocytes, (C and D) human fibroblasts, and (E and F) HUVEC. (G) Magnified image of SPACE peptide internalization in human keratinocytes. (H) Average fluorescence intensity of control peptide (open bars) and SPACE peptide (closed bars) internalization after 24 h in HUVEC, fibroblasts, and keratinocytes. Error bars indicate SD ($N \geq 30$). Scale bar: 100 μm (A–F) and 20 μm (G).

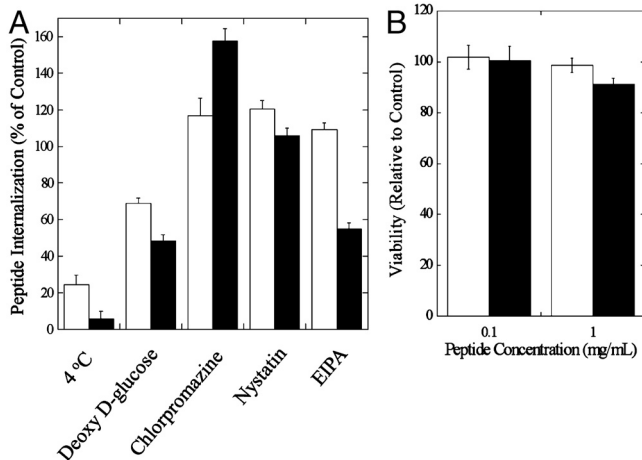


Fig. 3. Cellular mechanism and toxicity studies. (A) Peptide internalization (percent of control) for control peptide and SPACE peptide at 4 °C and with the endocytosis inhibitors deoxy-D-glucose, chlorpromazine, nystatin, and EIPA in human keratinocytes. (B) Cell proliferation of human keratinocytes in the presence of control peptide (open bars) or SPACE peptide (closed bars) at 0.1 mg/mL and 1.0 mg/mL. Error bars indicate SD ($N = 4$).

that neither SPACE peptide nor control peptide exhibited significant toxicity to cells at the concentration range studied here (0.1–1.0 mg/mL, Fig. 3B).

The ability of SPACE peptide to penetrate into a variety of cells makes it an excellent candidate for siRNA delivery. This possibility was explored using GFP-expressing endothelial cells as a model cell line in vitro. SPACE peptide-conjugated siRNA induced significant knockdown of GFP (Fig. 4A). In contrast, no significant knockdown was observed with siRNA alone, SPACE alone, SPACE conjugated to a control siRNA, or control peptide conjugated to siRNA. To determine whether siRNA conjugation to SPACE peptide had an adverse effect on the potency of siRNA, both unconjugated siRNA and SPACE-siRNA were complexed with Lipofectamine™ and knockdown was assessed. In both cases, knockdown was significant compared to control, that is, no siRNA treatment (Fig. S5 D–F).

SPACE peptide also penetrated into mouse skin in vivo at levels significantly higher than control peptide (Fig. S6 A–F, Fig. S7 A–F). Application of the SPACE peptide on mouse skin for 30 min resulted in penetration, and application for 2 h resulted in significant penetration into the skin and localization in the deep dermis, consistent with that seen in porcine and human skin.

The ability of SPACE peptide to enhance dermal penetration of IL-10 siRNA was next assessed. This siRNA was selected because of its potential for treating atopic dermatitis, a major dermatological disease. Because of the insignificant knockdown seen with control peptide and the lack of skin penetration in vivo when compared to SPACE peptide, the control peptide was not assessed in the in vivo siRNA studies. Application of IL-10 siRNA alone without the peptide produced minimal effect on IL-10 levels compared to mice that received no treatment, SPACE peptide alone, or SPACE conjugated to luciferase siRNA (control siRNA). In contrast, animals treated with SPACE conjugated to IL-10 siRNA and SPACE conjugated to 2-O-methyl modified IL-10 siRNA showed significant reduction in IL-10 levels (Fig. 4B).

As another example, SPACE peptide was conjugated to GAPDH siRNA and its effect on skin GAPDH levels was assessed. This target was chosen because GAPDH is a common housekeeping protein and provides an example of a common siRNA target. Animals treated with SPACE-GAPDH siRNA conjugate induced significant reduction in protein levels compared to controls (no treatment, siRNA alone, SPACE peptide

alone, and SPACE conjugated to control siRNA, Fig. 4C). Knockdown of GAPDH in skin was dose dependent; 43% knockdown was observed at 10 μM, 21% knockdown at 5 μM, and 10% knockdown at 1 μM (Fig. 4D). Knockdown was also dependent on application time with longer application times resulting in higher knockdown (Fig. S8).

Discussion

Penetration of phage across the SC is quite unexpected given its size (23–25). Large solutes (typically molecular mass > 500 Da) exhibit poor skin penetration and measurement of their transdermal permeation is often limited by the sensitivity of their detection. This limitation can be addressed by using phage. The M13 phage used in this study is a long filamentous particle, approximately 8 nm in width and 900 nm in length. High donor concentration ($\sim 2 \times 10^{11}$ pfu/mL), low detection limit (~ 1 pfu), and the potential for amplification facilitated assessment of dermal penetration of phage. The measured permeability of phage across porcine skin was very low; although the permeability of phage displaying SPACE peptide was higher than that of phage without the peptide library (see *SI Materials and Methods* for details). Permeation of phage, though much smaller than that of low molecular weight solutes, was significant and unexpected. Most importantly, penetration of phage was sequence-specific (see *SI Materials and Methods* for details).

Diffusion through intercellular lipids represents the classical mechanism for transdermal permeation of molecules. This mechanism, however, is generally limited to small, lipophilic molecules. Permeation of large, hydrophilic molecules is relatively less studied. Transdermal transport of such solutes is attributed to two pathways; (i) polar or porous pathways and (ii) appendages (follicles). Mathematical models have been described in the literature to describe contributions of both pathways to transdermal permeation (26, 27). Applications of these models to phage transport and their comparison with experimental observations is presented in *SI Materials and Methods*.

Deep penetration and retention of SPACE peptide in skin is very peculiar. A BLAST search revealed some matches to the SPACE peptide sequence including a complete match of the seven amino acid sequence to a protein in *Leishmania major* and a partial match (GSTQHQ) to a surface protein of skin-resident *Staphylococcus epidermidis*. The latter is of particular interest because the surface proteins dictate binding to extracellular matrix (ECM) components (28) and proteins that interact with ECM components may also interact with intermediate filaments such as keratin, a major component of skin (29). A few previous studies have used phage display to identify peptides that penetrate biological barriers including skin, oral mucosa, and lung epithelium. Chen et al. identified a peptide, TD-1 (AC-SSSPS-KH-CG), based on in vivo phage display on mouse skin (17). In another study, Kang et al. identified a sequence C-SKSSDYQ-C that enhances oral absorption after oral delivery of the phage library (30). More recently, Morris et al. studied translocation of phage library in alveolar epithelial cultures and identified a sequence C-TSGTHPR-C that enables translocation (31). The sequence of SPACE peptide shares some resemblance with the intestine-permeating peptide (note that T and S are similar). The SPACE peptide also shares some resemblance with the airway epithelium-penetrating peptide, especially in terms of the TGST motif.

The results presented here demonstrate the ability of the SPACE peptide to deliver siRNA across the SC and into skin cells at levels required to produce a therapeutic effect. Although several important siRNA therapeutic targets in skin have been identified, the delivery of siRNA into skin has proved challenging. This limitation can be potentially addressed through the studies reported here. Increased purity and optimization of the SPACE peptide-siRNA complex along with further studies

cysteines to produce a cyclic peptide. Fluorescein isothiocyanate (FITC) or 5-carboxyfluorescein (5-FAM) conjugated peptides were synthesized by ChinaTech Peptide Co. and RS Synthesis. The dye was placed on the N terminus of the peptide. Biotinylated versions of both peptides were synthesized by ChinaTech Peptide Co. and the peptides with no modifications were synthesized by RS Synthesis.

Peptide and Macromolecule Penetration in Skin. Full thickness porcine skin was obtained from the lateral abdominal region of Yorkshire pigs. Full thickness human skin was obtained from the National Disease Research Interchange. The skin was stored at -80°C and defrosted immediately prior to use. The conductivity of the skin was measured to ensure the integrity of the skin barrier. Skin samples with a resistivity above 50 k Ω were used for experiments. For fluorescently labeled peptides, 200 μL of a 1 mg/mL solution was placed in the donor compartment of the FDC. In the case of studying macromolecule delivery into skin, the peptide was first conjugated to the macromolecule (see *SI Materials and Methods*) and then the peptide-macromolecule complex was placed into the donor compartment of the FDC. After 24 h the remaining solution in the donor compartment was removed and the FDC was dismantled. The skin sample was retrieved and rinsed with deionized water to remove excess peptide or peptide complex on the surface of the skin. Skin samples were then prepared for imaging with confocal microscopy (see details in *SI Materials and Methods*).

Cell Penetration Studies. For cell penetration studies, 1.2×10^4 cells were seeded on poly-D-lysine-coated glass bottom culture dishes (MatTek). For human umbilical vein endothelial cells (HUVEC) cells, the culture dishes were coated with 1% gelatin prior to seeding with cells. After incubation at 37°C for 4 h, the media was removed and 20 μL of a 1 mg/mL fluorescent peptide solution was added to 180 μL of media and subsequently added to the cell culture dish. For the control, an equivalent amount of PBS was added in place of a peptide solution. After addition of the peptide, cell cultures were incubated at the appropriate condition for studying cellular penetration (4°C or 37°C) and incubated for either 6 or 24 h. Cells were prepared for imaging with confocal microscopy (see *SI Materials and Methods* for details).

Cell proliferation was measured using the Vybrant MTT Cell Proliferation Assay Kit (Invitrogen). Cells were incubated with various peptide solutions and cell proliferation was measured after 24 h.

Cell Penetration Mechanism Studies. For cell mechanism studies, cells were incubated with various endocytosis inhibitors or at 4°C for 1 h prior to the addition of fluorescently labeled peptides (see *SI Materials and Methods*). Cells were incubated with fluorescently labeled peptide for 3 h and then harvested for analysis using flow cytometry.

siRNA Delivery in Vitro. GFP-expressing endothelial cells (American Type Culture Collection) were grown in Dulbecco's modified Eagle's medium supplemented with 10% fetal bovine serum. GFP siRNA, 5'-GAC GUA AAC GGC CAC AAG UUC N6-3' (Dharmacon), was conjugated to fluorescently labeled peptide (containing a free carboxyl group) through *N*-(3-Dimethylaminopropyl)-*N'*-ethylcarbodiimide (EDC) chemistry (see *SI Materials and Methods* for details).

The peptide-siRNA complex was added to the appropriate cell culture media to obtain a final concentration of 1 μM siRNA. The media along with peptide-siRNA was then added to the cells and allowed to incubate for 48 h. Cells were imaged using confocal microscopy and image analysis was performed using ImageJ to determine the overall fluorescence intensity for each cell. Knockdown was determined as the percent of cells in the test case that possess intensity at least 30% lower than the mean intensity observed for the population in the control case (no treatment).

siRNA Delivery in Vivo. The siRNA sequences used in the in vivo studies are the following: IL-10, 5'-GAA UGA AUU UGA CAU CUU CUU N6-3'; GAPDH, 5'-GUG UGA ACC ACG AGA AAU AUU N6-3'; and luciferase (control), 5'-UAA GGC UAU GAA GAG AUA CUU N6-3'. The 2-O-methyl modification was placed on all bases for IL-10. All siRNAs were purchased from Dharmacon.

siRNA delivery was performed in female Balb/C mice (Charles River Laboratories) between six and eight-wk old according to protocols approved by the Institutional Animal Care and Use Committee. Mice were placed under anesthesia (1–2% isoflurane) and the hair on their back was lightly shaved. Two hundred microliters of a 10 μM of peptide-siRNA solution or corresponding controls were topically applied over a 3 cm^2 area on the back of the animal. The solution was then covered with sterile gauze and a breathable bandage. After 24 h for IL-10 experiments and 72 h for GAPDH experiments, the mice were euthanized using CO_2 and skin samples were immediately taken using a 4 mm biopsy punch. Two 4 mm biopsies were randomly taken from the treatment area and immediately frozen in liquid nitrogen. The skin was then placed in a surfactant combination of 0.5% (wt/vol) 3-(Decyl dimethyl ammonio) propane sulfonate (DPS) and Brij 30 and homogenized (IKA disperser) on ice for 1 min to extract the proteins from the skin samples. The homogenate was then centrifuged at 10,000 rpm for 5 min and the supernatant was collected. The total protein concentration was determined using the Micro Bicinchoninic Acid Protein Assay Kit (Pierce), IL-10 levels were determined using a mouse IL-10 ELISA (Raybiotech), and GAPDH levels were measured using the Kdalert™ GAPDH Assay kit (Ambion).

ACKNOWLEDGMENTS. Authors acknowledge Fred Tan and Jordanne Gregorio for technical assistance. This work was supported by the National Center for Research Resources shared instrumentation Grant 1S10RR017753-01.

- Nichols K, Cook-Bolden F (2009) Allergic skin disease: Major highlights and recent advances. *Med Clin North Am* 93:1211–1224.
- Koh H, Geller A (1995) Melanoma control in the United States: Current status. *Recent Results Cancer Res* 139:215–224.
- Fleischer AJ, Feldman S, Rapp S (2000) Introduction. The magnitude of skin disease in the United States. *Dermatol Clin* 18:15–21.
- Geusens B, Sanders N, Prow T, Van Gele M, Lambert J (2009) Cutaneous short-interfering RNA therapy. *Expert Opin Drug Delivery* 6:1333–1349.
- Prausnitz MR, Langer R (2008) Transdermal drug delivery. *Nat Biotechnol* 26:1261–1268.
- Guy R (2010) Transdermal drug delivery. *Handb Exp Pharmacol* (Marcel Dekker, Inc., New York), 2nd Ed., pp 399–410.
- Kigasawa K, et al. (2010) Noninvasive delivery of siRNA into the epidermis by iontophoresis using an atopic dermatitis-like model rat. *Int J Pharm* 383:157–160.
- Ritprajak P, Hashiguchi M, Azuma M (2008) Topical application of cream-emulsified CD86 siRNA ameliorates allergic skin disease by targeting cutaneous dendritic cells. *Mol Ther* 16:1323–1330.
- Mitragotri S, Blankschtein D, Langer R (1995) Ultrasound-mediated transdermal protein delivery. *Science* 269:850–853.
- Guy RH (1998) Iontophoresis—recent developments. *J Pharm Pharmacol* 50:371–374.
- Prausnitz MR (2004) Microneedles for transdermal drug delivery. *Adv Drug Delivery Rev* 56:581–587.
- Karande P, Jain A, Mitragotri S (2004) Discovery of transdermal penetration enhancers by high-throughput screening. *Nat Biotechnol* 22:192–197.
- Rothbard J, et al. (2000) Conjugation of arginine oligomers to cyclosporin A facilitates topical delivery and inhibition of inflammation. *Nat Med* 6:1253–1257.
- Lopes L, et al. (2005) Comparative study of the skin penetration of protein transduction domains and a conjugated peptide. *Pharm Res* 22:750–757.
- Sawant R, Torchilin V (2010) Intracellular transduction using cell-penetrating peptides. *Mol Biosyst* 6:628–640.
- Kim Y, Ludovice P, Prausnitz M (2007) Transdermal delivery enhanced by magainin pore-forming peptide. *J Controlled Release* 122:375–383.
- Chen Y, et al. (2006) Transdermal protein delivery by a coadministered peptide identified via phage display. *Nat Biotechnol* 24:455–460.
- Karande P, Jain A, Ergun K, Kispersky V, Mitragotri S (2005) Design principles of chemical penetration enhancers for transdermal drug delivery. *Proc Natl Acad Sci USA* 102:4688–4693.
- Nakase I, et al. (2004) Cellular uptake of arginine-rich peptides: Roles for macropinocytosis and actin rearrangement. *Mol Ther* 10:1011–1022.
- Patel LN, Zaro JL, Shen WC (2007) Cell penetrating peptides: Intracellular pathways and pharmaceutical perspectives. *Pharm Res* 24:1977–1992.
- Tamaru M, Akita H, Fujiwara T, Kajimoto K, Harashima H (2010) Leptin-derived peptide, a targeting ligand for mouse brain-derived endothelial cells via macropinocytosis. *Biochem Biophys Res Commun* 394:587–592.
- Walsh M, et al. (2006) Evaluation of cellular uptake and gene transfer efficiency of pegylated poly-L-lysine compacted DNA: Implications for cancer gene therapy. *Mol Pharm* 3:644–653.
- Potts RO, Guy RH (1992) Predicting skin permeability. *Pharm Res* 9:663–669.
- Magnusson B, Pugh W, Roberts M (2004) Simple rules defining the potential of compounds for transdermal delivery or toxicity. *Pharm Res* 21:1047–1054.
- Mitragotri S (2003) Modeling skin permeability to hydrophilic and hydrophobic solutes based on four permeation pathways. *J Controlled Release* 86:69–92.
- Tang H, Mitragotri S, Blankschtein D, Langer R (2001) Theoretical description of transdermal transport of hydrophilic permeants: Application to low-frequency sonophoresis. *J Pharm Sci* 90:545–568.
- Peck KD, Ghanem AH, Higuchi WI (1994) Hindered diffusion of polar molecules through and effective pore radii estimates of intact and ethanol treated human epidermal membrane. *Pharm Res* 11:1306–1314.
- Otto M (2009) *Staphylococcus epidermidis*—the accidental pathogen. *Nat Rev Microbiol* 7:555–567.
- Birkenfeld P, Haratz N, Klein G, Sulitzeanu D (1990) Cross-reactivity between the EBNA-1 p107 peptide, collagen, and keratin: Implications for the pathogenesis of rheumatoid arthritis. *Clin Immunol Immunopathol* 54:14–25.
- Kang SK, et al. (2008) Identification of a peptide sequence that improves transport of macromolecules across the intestinal mucosal barrier targeting goblet cells. *J Biotechnol* 135:210–216.

31. Morris CJ, Smith MW, Griffiths PC, McKeown NB, Gumbleton M (2011) Enhanced pulmonary absorption of a macromolecule through coupling to a sequence-specific phage display-derived peptide. *J Controlled Release* 151:83–94.
32. Leung DY (1995) Atopic dermatitis: The skin as a window into the pathogenesis of chronic allergic diseases. *J Allergy Clin Immunol* 96:302–318.
33. Palmer CN, et al. (2006) Common loss-of-function variants of the epidermal barrier protein filaggrin are a major predisposing factor for atopic dermatitis. *Nat Genet* 38:441–446.
34. Howell MD, et al. (2009) Cytokine modulation of atopic dermatitis filaggrin skin expression. *J Allergy Clin Immunol* 124((Suppl 2)):R7–R12.